ResearchGate

See discussions, stats, and author profiles for this publication at: https://www.researchgate.net/publication/356977688

Experimental Studies on the Relationship Between HDOP and Position Error in the GPS System

Article *in* Metrology and Measurement Systems · March 2022

DOI: 10.24425/mms.2022.138549

CITATIONS
11

READS
2,172

1 author:

Mariusz Specht
Gdynia Maritime University

190 PUBLICATIONS **1,535** CITATIONS

SEE PROFILE

All content following this page was uploaded by Mariusz Specht on 13 May 2022.

The user has requested enhancement of the downloaded file.

EXHIBIT
2003

www.czasopisma.pan.pl PAN www.journals.pan.pl

Metrol. Meas. Syst., Vol. 29 (2022) No. 1, pp. 17–36
DOI: 10.24425/mms.2022.138549

PAN POLSKA AKADEMIA NAUK

METROLOGY AND MEASUREMENT SYSTEMS

Index 330930, ISSN 0860-8229
www.metrology.wat.edu.pl

M&MS

EXPERIMENTAL STUDIES ON THE RELATIONSHIP BETWEEN HDOP AND POSITION ERROR IN THE GPS SYSTEM

Mariusz Specht

Department of Transport and Logistics, Gdynia Maritime University, Morska 81-87, 81-225 Gdynia, Poland,
(✉ *m.specht@wn.umg.edu.pl* +48 795 199 058)

Abstract

2D position error in the Global Positioning System (GPS) depends on the Horizontal Dilution of Precision (HDOP) and User Equivalent Range Error UERE. The non-dimensional HDOP coefficient, determining the influence of satellite distribution on the positioning accuracy, can be calculated exactly for a given moment in time. However, the UERE value is a magnitude variable in time, especially due to errors in radio propagation (ionosphere and troposphere effects) and it cannot be precisely predicted. The variability of the UERE causes the actual measurements (despite an exact theoretical mathematical correlation between the HDOP value and the position error) to indicate that position errors differ for the same HDOP value.

The aim of this article is to determine the relation between the GPS position error and the HDOP value. It is possible only statistically, based on an analysis of an exceptionally large measurement sample. To this end, measurement results of a 10-day GPS measurement campaign (900,000 fixes) have been used. For HDOP values (in the range of 0.6–1.8), position errors were recorded and analysed to determine the statistical distribution of GPS position errors corresponding to various HDOP values.

The experimental study and statistical analyses showed that the most common HDOP values in the GPS system are magnitudes of: 0.7 (p = 0.353) and 0.8 (p = 0.432). Only 2.77% of fixes indicated an HDOP value larger than 1. Moreover, 95% of measurements featured a geometric coefficient of 0.973 – this is why it can be assumed that in optimal conditions (without local terrain obstacles), the GPS system is capable of providing values of HDOP $\leq$ 1, with a probability greater than 95% (2σ). Obtaining a low HDOP value, which results in a low GPS position error value, calls for providing a high mean number of satellites (12 or more) and low variability in their number.

Keywords: Global Positioning System (GPS), Horizontal Dilution of Precision (HDOP), position error.

© 2022 Polish Academy of Sciences. All rights reserved

1. Introduction

The *Global Positioning System* (GPS) is currently the major positioning system used globally for purposes of determining location with all types of air [1–3], land [4–6] and marine [7–9] navigation and transportation applications. Moreover, this system is also used in many other

Copyright © 2022. The Author(s). This is an open-access article distributed under the terms of the Creative Commons Attribution-NonCommercial-NoDerivatives License (CC BY-NC-ND 4.0 https://creativecommons.org/licenses/by-nc-nd/4.0/), which permits use, distribution, and reproduction in any medium, provided that the article is properly cited, the use is non-commercial, and no modifications or adaptations are made.

Article history: received October 10, 2021; revised November 14, 2021; accepted November 18, 2021; available online December 11, 2021.

applications, *e.g.*, diagnostic [10, 11] and engineering [12, 13] measurements, scientific studies on the Earth and the environment [14, 15], also being an important element of time signal transmission systems [16, 17]. A special group of GPS users is constituted by individuals using personal navigation, which may be described as general purpose social navigation but connected with its non-professional applications, based on automotive location systems [18, 19] and mobile network [20, 21]. Both of these areas of GPS use, considering the number of users, are dominant today among all users of GPS navigation.

The main factor influencing the wide application possibilities of GPS is its high precision of determining location, which has increased over a few last decades. Data on GPS precision for determining position is regularly published by *United States Department of Defense* (U.S. DoD) in the form of standards as well as in other normative documents and it is also researched by many scientists. In 1993, GPS accuracy was 100 m ($p = 0.95$) horizontally [22]. In 2001, it increased to 13 m ($p = 0.95$) after turning off the *Selective Availability* (SA) [23]. Another change in positioning accuracy occurred in 2008 when it was 9 m ($p = 0.95$) [24]. In the following years, GPS accuracy kept changing and reached: 3.351 m in 2014 [25] and 1.891 m in 2017 [26].

The GPS positioning accuracy is measured with its error, which depends on three major types of measurement errors:

1. Errors caused by signal propagation, resulting from the ionospheric [27, 28] and tropospheric [29–31] effects, as well as errors caused by multipath [32, 33].
2. Errors caused by the space segment and connected with ephemeris errors, satellite clock errors as well as position errors stemming from the geometry of constellations [34, 35], represented by *Dilution of Precision* (DOP) coefficients [36, 37].
3. Instrument errors of receivers, which currently influence the precision of position determination to a limited extent [38, 39].

The relationship between the GPS position error and the indicated errors is based on the following relation [40]:

$$M = \sigma \cdot \mathrm{DOP}, \tag{1}$$

where: M – average position error [m], σ – measurement error of the navigation parameter (pseudorange) [m], DOP – geometric coefficient of the system's accuracy, depending on the spatial distribution of *Global Navigation Satellite System* (GNSS) satellites used in relation to the user [–].

It should be noted that the first section of the right-hand side of the equation UERE is the sum of errors in group 1 and errors of the space segment in group 2. Nevertheless, despite many publications and studies, its nature is complex and depends on numerous factors (among others, ionospheric and tropospheric effects). Modelling distance measurement errors in the GPS system have been presented in many publications. A model for GPS measurements (pseudorange) based on time series statistics was presented in [41]. Statistical modeling applied to the pseudorange in order to estimate the true satellite-user ranges, and therefore to reduce errors and to obtain information that allows service integrity monitoring was proposed in [42]. In [43] authors proposed improvements in accurate GPS positioning using the time series analysis.

Regarding the current paper, of high importance is the study carried out in [44]. In this article, Belabbas *et al.* measured the *Instantaneous Pseudo Range Error* (IPRE) as a sum of contributions of the error sources. These contributions are computed as a difference between estimated and reference values with one-year observation data received in several locations worldwide. The work highlights how considering a common and fixed standard deviation for any pseudorange can be quite a restricting approximation. In papers by various authors, especially [44, 45], it was shown that an analysis of the influence of the HDOP coefficient on the GPS position error, due

Page 3 of 21 (IPR2023-01374)
Google LLC et al v. Nariste Networks Pty. Ltd.

Metrol. Meas. Syst., Vol. 29 (2022), No. 1, pp. 17–36
DOI: 10.24425/mms.2022.138549

to the UERE value being difficult to be precisely estimated, should be carried out with statistical inference methods based on long measurement sessions. Moreover, it should be stressed that since the GPS system satellites constitute a constellation of various models built in different years, they feature varied technical characteristics, which significantly (and differently) influences the UERE value with respect to different satellites.

However, the second section of the Equation (1), being the DOP coefficient, is a non-dimensional coefficient describing the influence of satellite distribution against a receiver. It is determined in parallel with the position, as per known and widely used algorithms. It is also relatively simple to be modelled with the application of universally available and commonly used software for planning measurements [46–48], which, in turn, are widely used in geodesy and precision measurements. Depending on the dimension of the measured position and time, the DOP coefficients are divided into: GDOP (4D), PDOP (3D), HDOP (2D), VDOP (1D) and TDOP (1D).

The discussed analyses indicate that despite the possibilities of precise determination of the DOP value at a given moment of measurement and planning of the DOP values for any given moment of measurements, it is not currently possible to precisely determine at a given moment the average position error (M) due to the high number of unknown error components influencing the UERE value. Therefore, when planning GPS measurements to secure the highest possible positioning precision, only the value of the DOP coefficient is minimised through minimisation of the A matrix, the so-called DOP matrix, following the relation of [49, 50]:

$$\min\{trace(A)\} = \min\left\{trace\left[\left(G^T \cdot G\right)^{-1}\right]\right\} = \min\left\{\left[\frac{1}{|G|^2}\right]\sum_{i,j}\left(g'_{i,j}\right)^2\right\}. \tag{2}$$

This is determined based on a position line gradient matrix G (also called the matrix of coefficients or geometric matrix) [49, 50]:

$$A = \left(G^T \cdot G\right)^{-1}, \tag{3}$$

where: $g'_{i,j}$ – are elements of the matrix G^{-1}, provided G exists. From the presented relationship, it follows that it is possible to minimise the geometric coefficient by maximising the determinant of matrix G.

Another scalar-diagnostic used in the GPS system is the *Ambiguity Dilution of Precision* (ADOP), *i.e.* a predictor for carrier-phase ambiguity resolution performance [51]. However, the PDOP works well for code-based positioning, but one has to exercise great care in using it for *Real-Time Kinematic* (RTK) positioning. The use the ADOP, which is applicable to every GPS model in which ambiguities appear [52, 53].

As it has been shown, there is no firm relationship between the DOP value and the GPS position error. For this reason, it is only possible to determine this relation in an experiment and a measurement method combined. In connection with the above, this paper aimed to:

1. Account for conducting a long (10 days, with a frequency of 1 Hz) measurement session, using a typical (code) GPS receiver. For the analyses, 900,000 fixes were executed.
2. Show the results of the statistical analyses performed, making it possible to determine the average position error (M) with various HDOP values.
3. Determine which HDOP values occur the most often, which GPS position error distributions correspond to them (for a constant HDOP value) and the relation of this coefficient with the number of satellites.

It must be stressed that 900,000 fixes executed with the GPS system can be considered to be a representative sample for the study, which is research on statistical distributions of position errors. Previous analyses [54] showed that due to the GPS *Position Random Walk* (PRW), a sample consisting of approx. 78,000 measurements ensures statistics whose position error provides results similar to actual results obtained for a sample of approx. 1 million fixes.

The paper is divided into five parts. In Subsection 2.1, the relations are described between the GPS position error and its components and HDOP values. Subsection 2.2 contains a description of the methodology of measurement execution and information on surveys, their registration, data processing and the analysis methods. Section 3 presents study results and conclusions. In Section 4, the results are cross-referenced with other publications. The paper ends with final conclusions.

This is the fifth article in a series of monothematic publications "*Research on empirical (actual) statistical distributions of navigation system position errors*" [54–57]. The main scientific aim of this series is to answer the question of what statistical distributions follow the position errors of navigation systems such as GPS, *GLObal NAvigation Satellite System* (GLONASS), *BeiDou Navigation Satellite System* (BDS), Galileo, *Differential Global Positioning System* (DGPS), *European Geostationary Navigation Overlay Service* (EGNOS) and others. It must be emphasised that the purpose of both this paper and the whole series of publications is not to analyse the causes of PRW, such as ionospheric and tropospheric effects, multipath, noise, *etc.* This article rather analyses the statistical distributions of 1D and 2D position errors resulting from PRW. The causes might be very complex and probably deserve a separate series of publications.

2. Materials and Methods

2.1. Components of GPS Position Errors and DOP Value

The errors in group 1, as mentioned in the introduction, significantly influence the precision of a pseudo-distance measurement which is the distance between a receiver and a satellite containing receiver clock errors that cannot be precisely scheduled before measurements due to their spatial and temporal variability. The errors in group 2 are possible to be precisely modelled with commonly available software in the range of DOP values, but the ephemeris errors are connected, to a large extent, with the technical advancement of each satellite. The errors in group 2 may be estimated and transmitted in a navigation message in the form of the *User Range Accuracy* (URA) [58]. According to [59], the URA value is the standard deviation of the *User Range Error* (URE). However, the URE is determined based on the following relationship [60]:

$$\mathrm{URE} = \sqrt{(0.98R - T)^2 + 0.141^2\left(AT^2 + CT^2\right)}, \tag{4}$$

where: R – satellite radial error [m], T – satellite clock error [m], AT – satellite along-track error [m], CT – satellite cross-track error [m].

The GPS accuracy depends on the value of the selected DOP and the UERE, which includes both the URE and the *User Equipment Error* (UEE). The typical URE values are around 0.5-1 m and they depend on the GPS satellite block. However, the typical UEE value for today's receivers is about 1.6 m ($p = 0.95$) [61]. Therefore the above-presented formula for accuracy of position determination may be expressed in the following form [40]:

$$M = \mathrm{UERE} \cdot \mathrm{DOP} = \sqrt{\mathrm{URE}^2 + \mathrm{UEE}^2} \cdot \mathrm{DOP}, \tag{5}$$

Page 5 of 21 (IPR2023-01374)
Google LLC et al v. Nariste Networks Pty. Ltd.

Metrol. Meas. Syst., Vol. 29 (2022), No. 1, pp. 17–36
DOI: 10.24425/mms.2022.138549

where DOP coefficients are a measure of geometric conditions for determining position. This is a scalable value, describing the spatial distribution of objects against an observer. A detailed description of DOP coefficients is available in [40].

The essence of the DOP coefficient influence on position error in the GPS system is presented in Fig. 1. Two objects receive GPS signals, but the bus object features the possibility of receiving them from various directions and heights, thus the determination of position coordinates requires calculations based on position lines (position spheres, corresponding to distance measurements) which intersect at relatively large angles of close to 90° (α). On the other hand, the train object, due to signal terrain obstacles, *e.g.* the surrounding buildings, features no possibility to receive signals from various directions, thus the position lines intersect at small angles, spurring a high HDOP value, which results in a large position error.

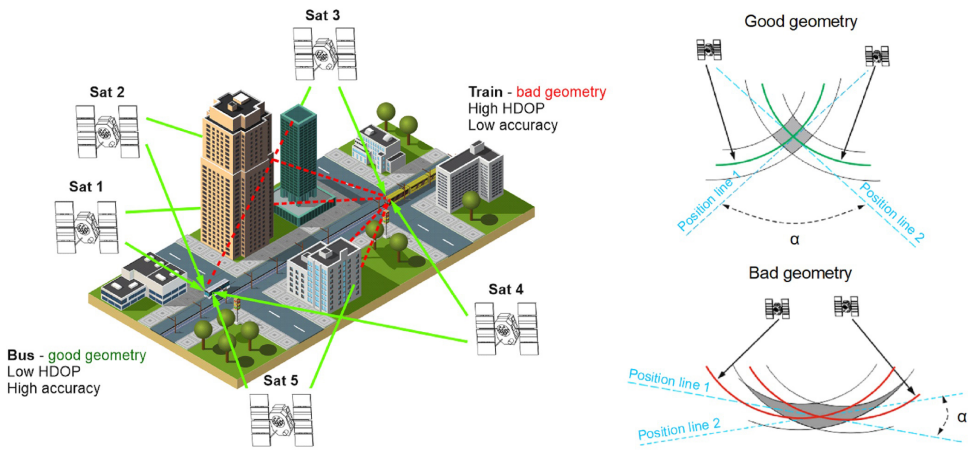

Fig. 1. Essence of the DOP coefficient influence on position error in the GPS system.

The process of calculating the DOP values for any given moment of measurements should begin with determining the coordinates of GPS satellites and the receiver in the *Earth-Centered, Earth-Fixed* (ECEF) coordinate system at the right moment in time, assuming that the satellite motion is described by Kepler's laws. To this end, the following data for each satellite should be obtained from the almanac files: mean anomaly at reference time, eccentricity, square root of the semi-major axis, longitude of ascending node of orbit plane at weekly epoch, inclination angle at reference time, argument of perigee, rate of right ascension and reference time ephemeris [59].

The next step is the transformation of satellites' coordinates from the ECEF system to the *East, North, Up* (ENU) system, determining their topocentric heights and omitting satellites with a negative value or less than the set value, and for the remaining ones, determining the azimuths measured from the receiver's position. Transformation matrix between ECEF-ENU systems, takes the form of [62]:

$$F = \begin{bmatrix} -\sin(L) & -\sin(B)\cdot\cos(L) & \cos(B)\cdot\cos(L) \\ \cos(L) & -\sin(B)\cdot\sin(L) & \cos(B)\cdot\sin(L) \\ 0 & \cos(B) & \sin(B) \end{bmatrix}, \tag{6}$$

where: B, L – receiver's coordinates [rad], which enables the calculation of satellite coordinates in the ENU system [62]:

$$\begin{bmatrix} X_{\mathrm{ENU}} \\ Y_{\mathrm{ENU}} \\ Z_{\mathrm{ENU}} \end{bmatrix} = F^T \cdot \begin{bmatrix} X_S - X_R \\ Y_S - Y_R \\ Z_S - Z_R \end{bmatrix}, \tag{7}$$

where: X_{ENU}, Y_{ENU}, Z_{ENU} – satellite coordinates in the ENU system [m], X_S, Y_S, Z_S – satellite coordinates in the ECEF system [m], X_R, Y_R, Z_R – receiver coordinates in the ECEF system [m], thus allowing to determine on their basis the elevation (topocentric height) of the satellite [61]:

$$El = \arctan\left(\frac{Z_{\mathrm{ENU}}}{\sqrt{X_{\mathrm{ENU}}^2 + Y_{\mathrm{ENU}}^2}}\right), \tag{8}$$

and its azimuth [61]:

$$Az = \begin{cases} \arctan\left(\left|\dfrac{X_{\mathrm{ENU}}}{Y_{\mathrm{ENU}}}\right|\right) & \text{for } X_{\mathrm{ENU}} \geq 0 \ \wedge \ Y_{\mathrm{ENU}} > 0 \\ \dfrac{\pi}{2} + \arctan\left(\left|\dfrac{Y_{\mathrm{ENU}}}{X_{\mathrm{ENU}}}\right|\right) & \text{for } X_{\mathrm{ENU}} > 0 \ \wedge \ Y_{\mathrm{ENU}} \leq 0 \\ \pi + \arctan\left(\left|\dfrac{X_{\mathrm{ENU}}}{Y_{\mathrm{ENU}}}\right|\right) & \text{for } X_{\mathrm{ENU}} \leq 0 \ \wedge \ Y_{\mathrm{ENU}} < 0 \\ \dfrac{3\pi}{2} + \arctan\left(\left|\dfrac{Y_{\mathrm{ENU}}}{X_{\mathrm{ENU}}}\right|\right) & \text{for } X_{\mathrm{ENU}} < 0 \ \wedge \ Y_{\mathrm{ENU}} \geq 0 \end{cases}. \tag{9}$$

And then, with the application of the line-of-sight matrix G [61]:

$$G = \begin{bmatrix} \cos(El_1) \cdot \sin(Az_1) & \cos(El_1) \cdot \cos(Az_1) & \sin(El_1) & 1 \\ \cos(El_2) \cdot \sin(Az_2) & \cos(El_2) \cdot \cos(Az_2) & \sin(El_2) & 1 \\ \vdots & \vdots & \vdots & \vdots \\ \cos(El_n) \cdot \sin(Az_n) & \cos(El_n) \cdot \cos(Az_n) & \sin(El_n) & 1 \end{bmatrix}, \tag{10}$$

where indexes $1 - n$ mean values for the next satellites, and a covariance matrix [61]:

$$A = \left(G^T \cdot G\right)^{-1} = \begin{bmatrix} A_{xx} & A_{xy} & A_{xz} & A_{xt} \\ A_{yx} & A_{yy} & A_{yz} & A_{yt} \\ A_{zx} & A_{zy} & A_{zz} & A_{zt} \\ A_{tx} & A_{ty} & A_{tz} & A_{tt} \end{bmatrix}. \tag{11}$$

DOP coefficients may be calculated [61]:

$$\mathrm{GDOP} = \sqrt{A_{xx} + A_{yy} + A_{zz} + A_{tt}}, \tag{12}$$

$$\mathrm{PDOP} = \sqrt{A_{xx} + A_{yy} + A_{zz}}, \tag{13}$$

$$\mathrm{HDOP} = \sqrt{A_{xx} + A_{yy}}, \tag{14}$$

$$\mathrm{VDOP} = \sqrt{A_{zz}}, \tag{15}$$

$$\mathrm{TDOP} = \sqrt{A_{tt}}. \tag{16}$$

Page 7 of 21 (IPR2023-01374)
Google LLC et al v. Nariste Networks Pty. Ltd.

Metrol. Meas. Syst., Vol. 29 (2022), No. 1, pp. 17–36
DOI: 10.24425/mms.2022.138549

2.2. Data processing

In the study, a typical (code) GPS receiver (Garmin GPS 19x HVS) was used, which worked in GPS mode, with a minimum topocentric height amounting to 10°. The selection of the receiver was intentional as it is a typical device and is widely used in navigation. The measurement was performed at coordinates: $\varphi = 54°29.973491'$N, $\lambda = 18°26.093580'$E (Gdynia, Poland). Earlier studies conducted on the representativeness of the GPS measurement session [54] showed that a measurement session of such a length is enough for a proper inference with respect to the precision characteristics of this system. The measurement results were transmitted through a serial port to a computer and stored there. In this way, a text file saved in the *National Marine Electronics Association* (NMEA) standard was obtained.

The results were processed in the following phases:

1. Verification of correctness of the saved measurement data, connected with the possibility of error occurrence in binary transmission between a computer and a receiver, resulting in errors in data. To this end, the author's own software was used which verifies the checksum for NMEA messages. GGA sentences that did not fulfil the requirement were removed.
2. The coordinates of ϕ and λ were transformed (with the Gauss–Krüger transformation) to plane coordinates $(x,\ y)$, expressed in metres, in line with mathematical relationships described in [63]. The transformation was executed using the Mathcad software and the author's own worksheets.
3. Generation of separate text files which contained the same values of the HDOP coefficient. As a result, 12 text files were created corresponding to HDOP values of: 0.6, 0.7, 0.8, 0.9, 1.0, 1.1, 1.2, 1.3, 1.4, 1.6, 1.7 and 1.8. The file for HDOP = 1.5 value was not created, as no measurement was recorded with this value.
4. Execution of statistical analysis of GPS position errors, separately for each of the 12 files. Arithmetic mean of geographic latitudes and longitudes, calculated for the entire sample, was assumed to be standard position. In Fig. 2, exemplary 2D position error distributions corresponding to HDOP values of: 0.6, 0.7, 0.8 and 0.9 are presented. The analyses were conducted using the Mathcad software.
5. The final stage of the study were statistical analyses of 2D position error distributions in GPS system measurements which were executed in the EasyFit software using the Mathcad software. To compare the statistical position error distributions, corresponding to various HDOP values (in the range of 0.6–1.0), the beta distribution was used. The study results [54, 56] showed that this distribution approximates the histograms of position errors of various systems, such as DGPS, GPS and EGNOS, very well while showing a high level of fitting. Position error distributions corresponding to various HDOP values will be approximated with the *Probability Density Function* (PDF) of the beta distribution, following this relation [64]:

$$f(x) = \frac{1}{B(\alpha_1, \alpha_2)} \frac{(x-a)^{\alpha_1 - 1}(b-x)^{\alpha_2 - 1}}{(b-a)^{\alpha_1 + \alpha_2 - 1}}, \tag{17}$$

$$B(\alpha_1, \alpha_2) = \int_0^1 t^{\alpha_1 - t}(1-t)^{\alpha_2 - t}\,\mathrm{d}t, \tag{18}$$

where: α_1 – continuous shape parameter ($\alpha_1 > 0$), α_2 – continuous shape parameter ($\alpha_2 > 0$), a, b – continuous boundary parameters ($a < b$), $B(\alpha_1, \alpha_2)$ – beta function.

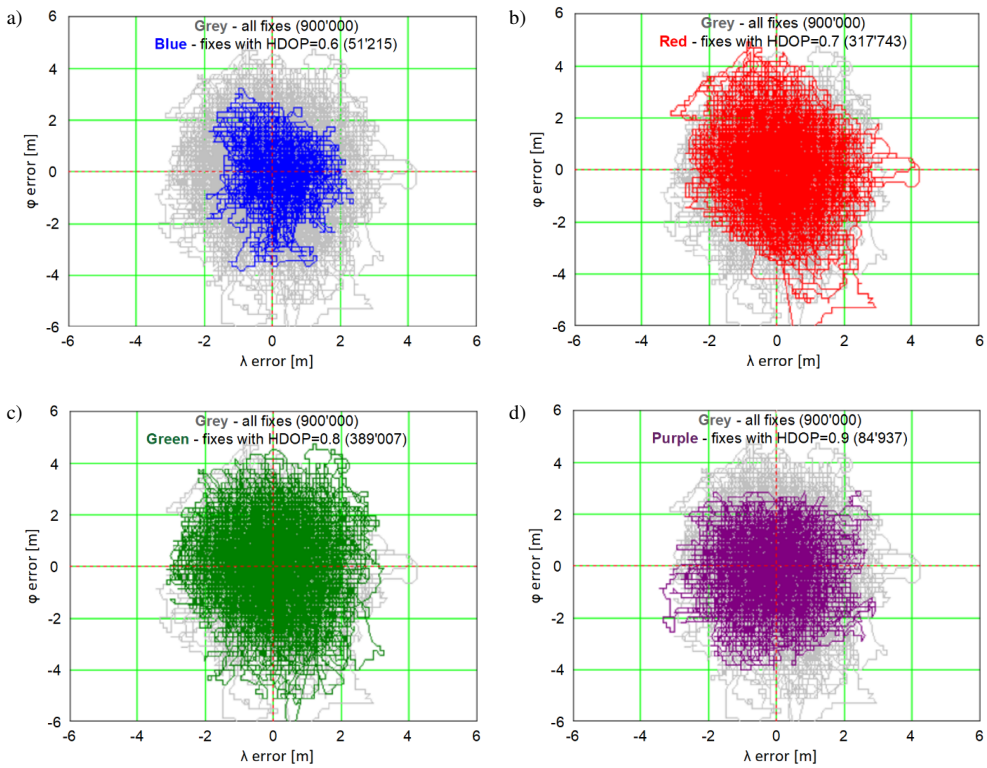

Fig. 2. Exemplary 2D position error distributions corresponding to HDOP values of: 0.6 (a), 0.7 (b), 0.8 (c) and 0.9 (d).

3. Results

The first phase of statistical analyses of HDOP value variability was to determine the descriptive statistics for this variable. To that purpose, statistical measure values were determined for all performed fixes. Based on this, it will be further possible to analyse 2D position errors for each HDOP value separately. For the purpose of analyses, only those measures (arithmetic mean, kurtosis, quantiles, range, skewness, standard deviation and variance) were selected for which the values are tightly related with the 2D position error. The substantiation and significance of these measures in a statistical analysis of position error distributions have been described previously [54, 56] and will not be discussed in this paper. In Table 1, descriptive statistics are presented for the entire population of the measured positions (900,000 fixes) along with two charts: *Cumulative Distribution Function* (CDF) and PDF.

Table 1 shows the following general conclusions:

– HDOP value distribution is a right-skewed (asymmetrical) with a mean HDOP value amounting to 0.781, with a relatively low standard deviation of 0.113. HDOP value kurtosis is leptokurtic (*Kurt* >0), which means that it is more concentrated around the mean value than the normal distribution would suggest.

– The most common HDOP values are 0.7 and 0.8, considerably influencing the statistics of all HDOP values.

Page 9 of 21 (IPR2023-01374)
Google LLC et al v. Nariste Networks Pty. Ltd.

Metrol. Meas. Syst., Vol. 29 (2022), No. 1, pp. 17–36
DOI: 10.24425/mms.2022.138549

– The mean HDOP value is relatively low, which is connected with, above all, the optimal conditions for executing measurements, there were no terrain obstacles.
– It must be stressed that 95% of fixes featured a geometric coefficient lower than or equalling 1. It may be assumed that in optimal conditions (without local terrain obstacles), the GPS system is capable of providing values of HDOP $\leq$ 1, with a probability greater than 95% (2σ).

Table 1. HDOP value statistical measures in GPS measurements (900,000 fixes).

Descriptive statistic	*HDOP* value	Function
Sample size	900,000	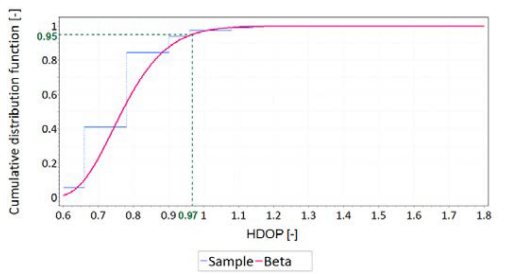
Arithmetic mean	0.781	
Range	1.2	
Variance	0.013	
Standard deviation	0.113	
Skewness	2.147	
Kurtosis	10.876	
Min. percentile	0.6	
5th percentile	0.6	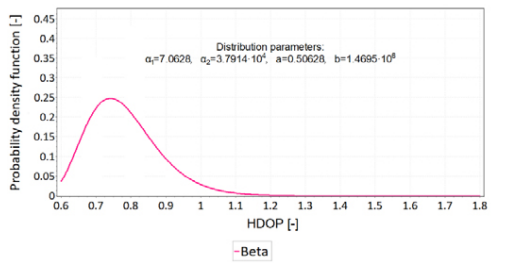
10th percentile	0.7	
25th percentile (Q1)	0.7	
50th percentile (Median)	0.8	
75th percentile (Q3)	0.8	
90th percentile	0.9	
95th percentile	1	
Max percentile	1.8	

The bottom section of Table 1 features percentile statistics for the entire population, which are used (discussed) in a subsequent part of the paper – with statistical analysis performed for each HDOP value separately.

Subsequently, analysis of the availability of a given HDOP value in the function of time was performed. Thus, it required a measurement method to determine the percentage of time in which the individual values of this coefficient occurred. In Fig. 3a, the percentage distribution of HDOP

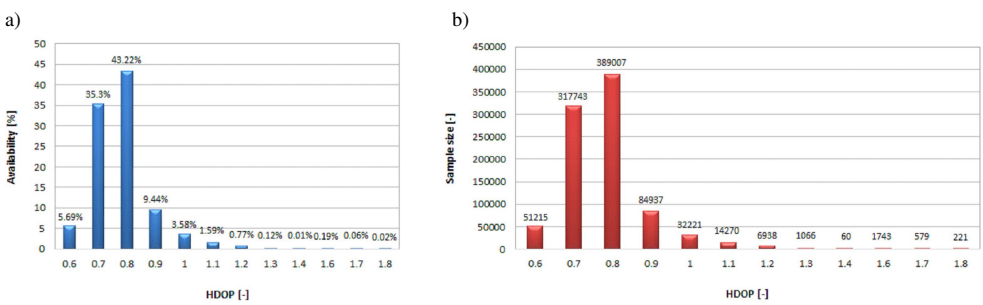

Fig. 3. Availability (a) and sample size (b) of individual HDOP values (in the range of 0.6–1.8).

values (in the range of 0.6–1.8) is presented. At the same time, in Fig. 3b, the sample size is presented for sets of individual coefficients (sets with the same value of the HDOP coefficient).

Charts presented in Fig. 3 prove that:

– The most common HDOP values are 0.7 and 0.8. In total, they occur 78.52% of the time.
– The occurrence probability of HDOP values exceeding 1 amounts to merely 2.77% and this needs to be considered very low.

Large measurement numbers (Fig. 3b), corresponding to values of HDOP = 0.7 and HDOP = 0.8 and amounting to 317,743 and 389,007 fixes, respectively, as well as the large size of sets (for HDOP values in the range of 0.6–1.0) justify the execution of further analyses and inference regarding 2D position errors, especially for these values. The size of the remaining sets (for HDOP values in the range of 1.1–1.8) is relatively low. Owing to this, any inference regarding these statistics should be considered unrepresentative.

A feature of GNSS systems is the change of satellite position against a receiver located on the Earth. Its result is the number of satellites, variable in time, used for determining position. It causes a constant change of HDOP values for a GPS receiver and, thus, a change in its position error. To simplify the matter, it can be assumed that when more satellites are used for determining position, the position error should be smaller (in a statistical approach). Of course, their position in relation to a receiver also plays an important role. It can be concluded that a large number of satellites greatly increases the occurrence probability of their favourable distribution against the user's receiver, resulting in a small position error. For this reason, in the next phase of the research, *i.e.* HDOP statistical analysis, the number of satellites should be the subject of a study corresponding to given HDOP values. However, there are two more factors which still need to be determined: the mean number of satellites for each of the considered HDOP values (in the range of 0.6–1.0) and the variability of the number of satellites (from the statistical point of view).

To address these issues, separate sets were created by sorting the results corresponding to HDOP values amounting to: 0.6, 0.7, 0.8, 0.9 and 1.0 secured, due to their representativeness, by a large number of fixes. To provide scientific reliability, analyses for the example non-representative HDOP values of 1.3 and 1.6 will be presented. However, the small number of measurements for both of these values is insufficient for making generalised conclusions.

The charts presented in Fig. 4 feature important differentiation of statistical measure values which are shown in Table 2.

Results presented in Fig. 4 and Table 2 lead to the following conclusions:

– The highest value of HDOP = 0.6 was provided by a GPS constellation consisting of 12, 13, 14, 15 and 16 satellites, of which the value of 14 is predominant. The mean number of satellites was high (14.085), with a relatively small standard deviation of 0.76, which must be emphasised. HDOP value distribution is a right-skewed (weakly asymmetrical) and the skewness is leptokurtic ($Kurt > 0$).
– To obtain a coefficient value of HDOP = 0.7 ($p = 0.353$), 9, 10, 11, 12, 13 and 14 satellites were used. The most common was the use of 13 satellites. The mean number of satellites amounted to 12.506, with a standard deviation of 1.063. This is a value almost one and a half times higher than in the case of HDOP = 0.6. HDOP value distribution is a left-skewed (very weakly asymmetrical) and the skewness is platykurtic ($Kurt < 0$).
– The most commonly occurring value of HDOP = 0.8 ($p = 0.432$) was ensured with the use of 8, 9, 10, 11, 12, 13 and 14 satellites. The most common was the use of 11 satellites. The mean number of satellites amounted to 11.336, with a standard deviation of 1.04 – similar to that of HDOP = 0.7. HDOP value distribution is a right-skewed (very weakly asymmetrical) and the skewness is platykurtic ($Kurt < 0$).

Page 11 of 21 (IPR2023-01374)
Google LLC et al v. Nariste Networks Pty. Ltd.

Metrol. Meas. Syst., Vol. 29 (2022), No. 1, pp. 17–36
DOI: 10.24425/mms.2022.138549

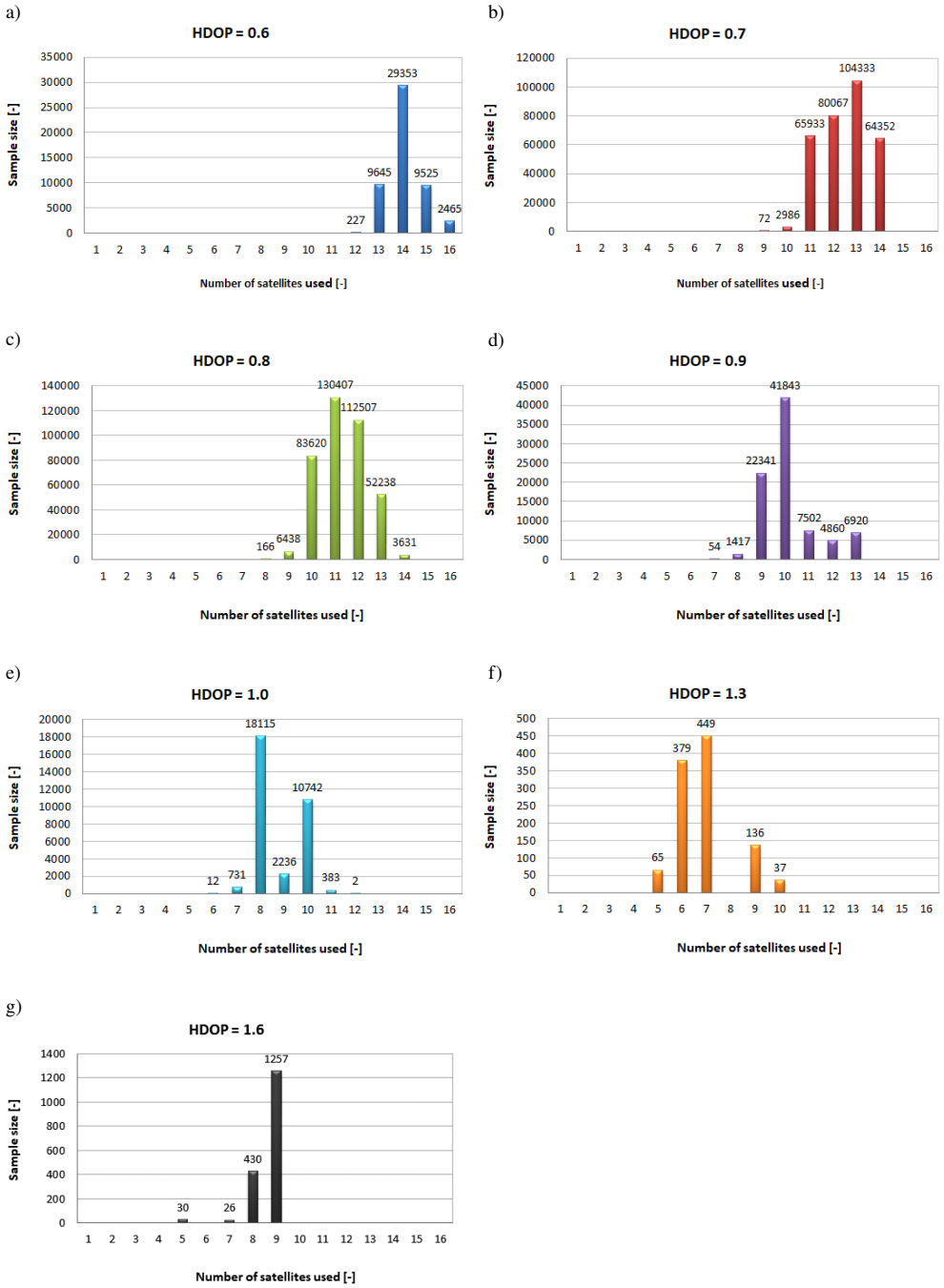

Fig. 4. The number of satellites ensuring constant value of the HDOP coefficient [for the value of: 0.6 (a), 0.7 (b), 0.8 (c), 0.9 (d) and 1.0 (e)]. Additionally, the charts have been supplemented with non-representative (due to the small population size) results for HDOP = 1.3 (f) and HDOP = 1.6 (g)

– For the remaining HDOP values of 0.9 and 1.0, an evident decrease in the mean number of satellites is visible, amounting to 10.149 satellites and 8.749 satellites, respectively. HDOP value distributions are right-skewed (weakly asymmetrical) and their skewness is leptokurtic (HDOP = 0.9) or platykurtic (HDOP = 1.0).

Table 2. Statistical measures regarding the sets of GPS satellite numbers, featuring identical HDOP values.

Descriptive statistic	**Number of satellites**				
	HDOP = 0.6	**HDOP = 0.7**	**HDOP = 0.8**	**HDOP = 0.9**	**HDOP = 1.0**
Sample size	51,215	317,743	389,007	84,937	32,221
Availability	5.69%	35.30%	43.22%	9.44%	3.58%
Arithmetic mean	14.085	12.506	11.336	10.149	8.749
Range	4	5	6	6	6
Variance	0.577	1.129	1.082	1.364	0.975
Standard deviation	0.76	1.063	1.04	1.168	0.987
Skewness	0.454	–0.155	0.112	0.115	0.444
Kurtosis	0.368	–1.025	–0.617	0.004	–1.379
Min. percentile	12	9	8	7	6
5th percentile	13	11	10	9	8
10th percentile	13	11	10	9	8
25th percentile (Q1)	14	12	11	9	8
50th percentile (Median)	14	13	11	10	8
75th percentile (Q3)	14	13	12	10	10
90th percentile	15	14	13	12	10
95th percentile	15	14	13	13	10
Max percentile	16	14	14	13	12

Another element of the study was the evaluation of positioning precision, corresponding to given HDOP values. The first phase in the search of relationships between HDOP values and position error was the evaluation of GPS position errors over the entire measurement session (900,000 fixes) (Table 3).

Table 3. GPS position error statistics, determined for the entire measurement session (900,000 fixes).

Descriptive statistic	**2D position error**	**PDF for 2D position error**	**2D position error distribution**
Sample size	900,000	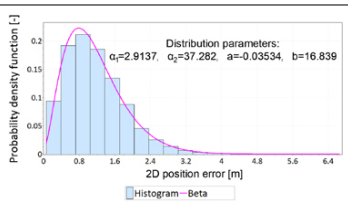	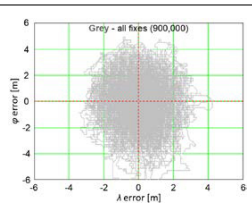
Arithmetic mean	0.875 m		
Range	0.802 m		
Variance	5.993 m		
Standard deviation	2.448 m		
R95	2.393 m		

The results presented in Table 3 are typical for the GPS system, which is evidenced by R95, *i.e.* radius of sphere centred at the true position, containing the position estimate with probability of 95%, amounting to 2.393 m. The results are the basis for subsequent analyses of positioning precision, regarding individual HDOP values separately.

Metrol. Meas. Syst., Vol. 29 (2022), No. 1, pp. 17–36
DOI: 10.24425/mms.2022.138549

Following the presented procedure (described in Subsection 2.2), a statistical analysis of GPS position error values was conducted for sets containing the same HDOP value. In Table 4, cumulative results are presented for the determination of positioning precision, as provided for with individual, variable HDOP values (in the range of 0.6–1.0). The most important measure is R95, defined for the set of measurements featuring identical HDOP values.

Table 4. Statistical analyses of GPS position error sets for a given HDOP value (in the range of 0.6–1.0).

Descriptive statistic	**2D position error**				
	HDOP = 0.6	**HDOP = 0.7**	**HDOP = 0.8**	**HDOP = 0.9**	**HDOP = 1.0**
Sample size	51,215	317,743	389,007	84,937	32,221
Availability	5.69%	35.30%	43.22%	9.44%	3.58%
Arithmetic mean	0.988 m	1.16 m	1.151 m	1.168 m	1.353 m
Range	3.902 m	6.582 m	6.582 m	4.109 m	6.102 m
Variance	0.322 m	0.41 m	0.439 m	0.456 m	0.673 m
Standard deviation	0.568 m	0.641 m	0.663 m	0.675 m	0.82 m
R95	2.048 m	2.31 m	2.373 m	2.493 m	2.889 m

Owing to a considerable number of fixes, Table 4 includes only data that can be considered statistically representative, the same is not the case for data presented in Table 5, which refer to HDOP values in the range of 1.1–1.8. It can be seen that the position error for HDOP value between 0.6 and 1.0 increases, which is an expected phenomenon. However, in the case of data in Table 5, it is visible that the value of R95 measure is decreasing, which is irrational. It seems that a number of fixes is by far insufficient for statistical inference, and the PRW [54] occurring in the GPS system additionally favours a low error value for small measurement samples.

Table 5. Statistical analyses of GPS position error sets for a given HDOP value (in the range of 1.1–1.8).

Descriptive statistic	**2D position error**						
	HDOP = 1.1	**HDOP = 1.2**	**HDOP = 1.3**	**HDOP = 1.4**	**HDOP = 1.6**	**HDOP = 1.7**	**HDOP = 1.8**
Sample size	14,270	6938	1066	60	1743	579	221
Availability	1.59%	0.77%	0.12%	0.01%	0.19%	0.06%	0.02%
Arithmetic mean	1.082 m	1.18 m	1.561 m	0.796 m	1.305 m	1.356 m	1.54 m
Range	4.38 m	4.393 m	3.545 m	1.001 m	4.416 m	3.216 m	2.302 m
Variance	0.398 m	0.46 m	0.602 m	0.069 m	0.568 m	0.582 m	0.424 m
Standard deviation	0.631m	0.678 m	0.776 m	0.263 m	0.754 m	0.763 m	0.651 m
R95	2.208 m	2.438 m	3.095 m	1.284 m	2.71 m	2.631 m	2.483 m

4. Discussion

The study discussed in this paper was conducted in optimal conditions for tracking GPS signals as there were no terrain obstacles around the receiver. That is why a very high number of fixes featured a low HDOP (with values of 0.7 and 0.8) in the researched sample of 900,000

measurements. More precisely, the low value of this coefficient and the large number of fixes featuring low HDOP values resulted in the value of the R95 measure for the entire campaign reaching the value of 2.393 m, which should be considered low. Moreover, it is interesting that only 2.77% of measurements feature values of HDOP > 1, which means that if they are free of coarse and outstanding errors, they do not influence the value of the R95 measure for the entire population in any considerable way.

In typical GPS usage conditions in land navigation (car navigation systems, geodesy, smartphones, *etc.*), where terrain obstacles are practically permanently present, obtaining such a high precision would not be possible. Thus, it should not be expected to obtain similar results in practical use with this type of navigation. However, with air and marine navigation, where there are practically no obstacles to GPS signals, one may expect similar results in practical applications.

In Fig. 5, GPS position error values are correlated with corresponding HDOP values. For each HDOP value, a separate function was drawn for the position error PDF which featured constant values of HDOP (in the range of 0.6–1.0). PDFs were drawn based on approximation of GPS position errors with the probability density function of the beta distribution, which features very good fitting with navigation positioning system errors due to its highly universal characteristics [56]. Fig. 5 was supplemented with R95 values, determined separately for each set of position errors, defined for constant values of HDOP.

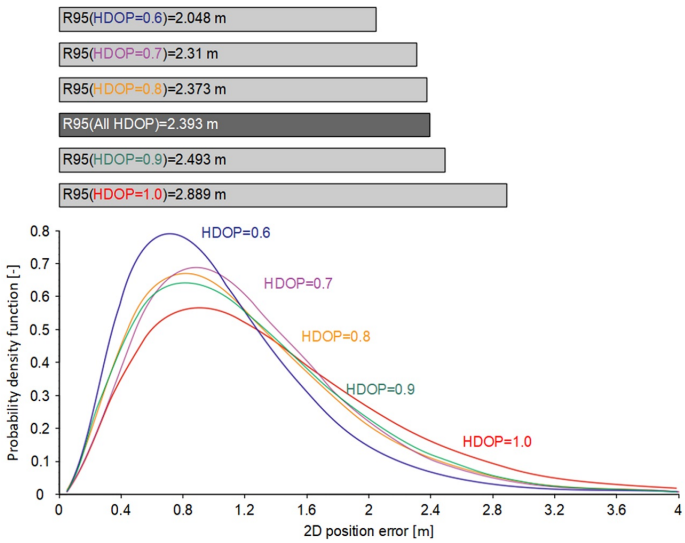

Fig. 5. GPS position error PDFs, determined separately for HDOP values (in the range of 0.6–1.0), together with R95 measures, calculated separately for measurements with a constant HDOP value.

To spot regularities in Fig. 5, it is justifiable to compare extreme figures, *i.e.* for HDOP = 0.6 and HDOP = 1.0. The position error value calculated for a sample featuring HDOP = 0.6 is 2.048 m, which means it amounts to 85.58% of the R95 value out of the entire measurement population and it is almost 1 metre smaller than the R95 measure determined for the HDOP = 1.0 set. It should be stressed that the condition for maintaining a low HDOP value is the need to provide for a large number of satellites (mean of 14.085) with a very small standard deviation of 0.76 for HDOP = 0.6. Moreover, the range of this set was 4 satellites. However, in the

Metrol. Meas. Syst., Vol. 29 (2022), No. 1, pp. 17–36
DOI: 10.24425/mms.2022.138549

case of the HDOP = 1.0 value, one can notice a lower mean number of satellites (8.749) with a higher standard deviation and range increase from 4 (HDOP = 0.6) to 6 (HDOP = 1.0). These differences conditioned a situation in which the R95 measure for measurements featuring the value of HDOP = 1.0 may exceed the R95 value by 50 cm, as calculated for the entire population.

5. Conclusions

This paper analysed the statistical evaluation of the influence of the HDOP value on the 2D position error in the GPS system, represented by R95 measure. The main factors influencing the position error in the GPS system are values of HDOP and UERE. The variability of the UERE causes the actual measurements (despite an exact theoretical mathematical correlation between HDOP value and the 2D position error) to indicate that 2D position errors differ for the same HDOP value. Although it is currently impossible to model the UERE value precisely, an evaluation of DOP influence on the position error in the GPS system can be carried out based on an experimental and measurement approach.

The experimental study and statistical analyses showed that the most common HDOP values in the GPS system are magnitudes of: 0.7 ($p = 0.353$) and 0.8 ($p = 0.432$). Only 2.77% of fixes indicated an HDOP value larger than 1. Moreover, 95% of measurements featured a geometric coefficient of 0.973 – this is why it can be assumed that in optimal conditions (without local terrain obstacles), the GPS system is capable of providing values of HDOP ≤ 1, with a probability greater than 95% (2σ). Obtaining a low HDOP value, which results in a low GPS position error value, calls for providing a high mean number of satellites (12 or more) and low variability in their number.

The study has shown that the method widely used in navigation for determining 2D position error value based on multiplication of the HDOP value (by mean UERE value) can only be considered an approximate estimation accuracy.

Acknowledgements

This research was funded from the statutory activities of Gdynia Maritime University, grant number WN/2021/PZ/05.

References

[1] Krasuski, K., Ciećko, A., Bakuła, M., & Wierzbicki, D. (2020). New Strategy for Improving the Accuracy of Aircraft Positioning Based on GPS SPP Solution. *Sensors*, *20*(17), 4921. https://doi.org/10.3390/s20174921

[2] Lachapelle, G., Cannon, M. E., Qiu, W., & Varner, C. (1996). Precise Aircraft Single-point Positioning Using GPS Post-mission Orbits and Satellite Clock Corrections. *Journal of Geodesy*, *70*(9), 562–571. https://doi.org/10.1007/bf00867864

[3] Ochieng, W. Y., Sauer, K., Walsh, D., Brodin, G., Griffin, S., & Denney, M. (2003). GPS Integrity and Potential Impact on Aviation Safety. *The Journal of Navigation*, *56*(1), 51–65. https://doi.org/10.1017/S0373463302002096

[4] Elhajj, M., & Ochieng, W. (2020). Impact of New GPS Signals on Positioning Accuracy for Urban Bus Operations. *The Journal of Navigation*, *73*(6), 1284–1305. https://doi.org/10.1017/S0373463320000272

[5] Naranjo, J. E., Jiménez, F., Aparicio, F., & Zato, J. (2009). GPS and Inertial Systems for High Precision Positioning on Motorways. *The Journal of Navigation*, *62*(2), 351–363. https://doi.org/10.1017/S0373463308005249

[6] Sun, Q. C., Odolinski, R., Xia, J. C., Foster, J., Falkmer, T., & Lee, H. (2017). Validating the Efficacy of GPS Tracking Vehicle Movement for Driving Behaviour Assessment. *Travel Behaviour and Society*, *6*, 32–43. https://doi.org/10.1016/j.tbs.2016.05.001

[7] Bhatti, J., & Humphreys, T. E. (2017). Hostile Control of Ships via False GPS Signals: Demonstration and Detection. *NAVIGATION, Journal of the Institute of Navigation*, *64*(1), 51–66. https://doi.org/10.1002/navi.183

[8] Glomsvoll, O., & Bonenberg, L. K. (2017). GNSS Jamming Resilience for Close to Shore Navigation in the Northern Sea. *The Journal of Navigation*, *70*(1), 33–48. https://doi.org/10.1017/S0373463316000473

[9] Han, J., Park, J., Kim, J., & Son, N.-S. (2016). GPS-less Coastal Navigation Using Marine Radar for USV Operation. *IFAC-PapersOnLine*, *49*(23), 598–603. https://doi.org/10.1016/j.ifacol.2016.10.500

[10] Gao, Z., Ge, M., Li, Y., Shen, W., Zhang, H., & Schuh, H. (2018). Railway Irregularity Measuring Using Rauch–Tung–Striebel Smoothed Multi-sensors Fusion System: Quad-GNSS PPP, IMU, Odometer, and Track Gauge. *GPS Solutions*, *22*(2), 36. https://doi.org/10.1007/s10291-018-0702-5

[11] Specht, C., Koc, W., Chrostowski, P., & Szmagliński, J. (2019). Accuracy Assessment of Mobile Satellite Measurements in Relation to the Geometrical Layout of Rail Tracks. *Metrology and Measurement Systems*, *26*(2), 309–321. https://doi.org/10.24425/mms.2019.128359

[12] Kizil, U., & Tisor, L. (2011). Evaluation of RTK-GPS and Total Station for Applications in Land Surveying. *Journal of Earth System Science*, *120*, 215–221. https://doi.org/10.1007/s12040-011-0044-y

[13] Liu, C., Gao, J. X., Yu, X. X., Zhang, J. X., & Zhang, A. B. (2015). Mine Surface Deformation Monitoring Using Modified GPS RTK with Surveying Rod: Initial Results. *Survey Review*, *47*(341), 79–86. https://doi.org/10.1179/1752270614Y.0000000092

[14] Contreras-de-Villar, F., García, F. J., Muñoz-Perez, J. J., Contreras-de-Villar, A., Ruiz-Ortiz, V., Lopez, P., Garcia-López, S., & Jigena, B. (2021). Beach Leveling Using a Remotely Piloted Aircraft System (RPAS): Problems and Solutions. *Journal of Marine Science and Engineering*, *9*(1), 19. https://doi.org/10.3390/jmse9010019

[15] Stateczny, A., Gronska-Sledz, D., & Motyl, W. (2019). Precise Bathymetry as a Step Towards Producing Bathymetric Electronic Navigational Charts for Comparative (Terrain Reference) Navigation. *The Journal of Navigation*, *72*(6), 1623–1632. https://doi.org/10.1017/S0373463319000377

[16] Lewandowski, W., & Thomas, C. (1991). GPS Time Transfer. *Proceedings of the IEEE*, *79*(7), 991–1000. https://doi.org/10.1109/5.84976

[17] Lombardi, M. A., Nelson, L. M., Novick, A. N., & Zhang, V. S. (2001). Time and Frequency Measurements Using the Global Positioning System (GPS). *CAL LAB: The International Journal of Metrology*, *8*, 26–33. https://tsapps.nist.gov/publication/get_pdf.cfm?pub_id=105004

[18] Lee, Y.-S., Park, J.-H., & Kim, S.-K. (2009). Applying Embedded System Forensics to Car GPS Navigation System Analysis. *The Journal of Advanced Navigation Technology*, *13*(5), 639–645. https://www.koreascience.or.kr/article/JAKO200919663061368.page

[19] Uradziński, M., Rapiński, J., Tomaszewski, D., Śmieja, M., Guo, H., Yu, S., & Jian, X. (2017). Assessment of Usefulness of the MEMS-based Integrated Navigation Unit in Car Navigation. *Technical Sciences*, *20*(4), 321–331. https://doi.org/10.31648/ts.5430

Metrol. Meas. Syst., Vol. 29 (2022), No. 1, pp. 17–36
DOI: 10.24425/mms.2022.138549

[20] Li, G., & Geng, J. (2019). Characteristics of Raw Multi-GNSS Measurement Error from Google Android Smart Devices. *GPS Solutions*, *23*(3), 90. https://doi.org/10.1007/s10291-019-0885-4

[21] Paziewski, J. (2020). Recent Advances and Perspectives for Positioning and Applications with Smartphone GNSS Observations. *Measurement Science and Technology*, *31*(9), 091001. https://doi.org/10.1088/1361-6501/ab8a7d

[22] U.S. DoD. (1993). *Global Positioning System Standard Positioning Service Signal Specification*. U.S. DoD. https://www.gps.gov/technical/ps/1993-SPS-signal-specification.pdf

[23] U.S. DoD. (2001). *Global Positioning System Standard Positioning Service Performance Standard*. U.S. DoD. https://www.navcen.uscg.gov/pdf/gps/geninfo/2001SPSPerformanceStandardFINAL.pdf

[24] U.S. DoD. (2008). *Global Positioning System Standard Positioning Service Performance Standard*. U.S. DoD. https://www.gps.gov/technical/ps/2008-SPS-performance-standard.pdf

[25] FAA William J. Hughes Technical Center (2020). *Global Positioning System (GPS) Standard Positioning Service (SPS) Performance Analysis Report*. FAA William J. Hughes Technical Center. https://www.nstb.tc.faa.gov/reports/2020_Q3_SPS_PAN111_v1.0.pdf

[26] Renfro, B. A., Stein, M., Boeker, N., & Terry, A. (2018). *An Analysis of Global Positioning System (GPS) Standard Positioning Service (SPS) Performance for 2017*. SGL. https://www.gps.gov/systems/gps/performance/2017-GPS-SPS-performance-analysis.pdf

[27] Akgul, V., Gurbuz, G., Kutoglu, S. H., & Jin, S. (2020). Effects of the High-order Ionospheric Delay on GPS-based Tropospheric Parameter Estimations in Turkey. *Remote Sensing*, *12(21)*, 3569. https://doi.org/10.3390/rs12213569

[28] Liu, Z., Li, Y., Guo, J., & Li, F. (2016). Influence of Higher-order Ionospheric Delay Correction on GPS Precise Orbit Determination and Precise Positioning. *Geodesy and Geodynamics*, *7*(5), 369–376. https://doi.org/10.1016/j.geog.2016.06.005

[29] Renga, A., Causa, F., Tancredi, U., & Grassi, M. (2018). Accurate Ionospheric Delay Model for Real-time GPS-based Positioning of LEO Satellites Using Horizontal VTEC Gradient Estimation. *GPS Solutions*, *22*(2), 46. https://doi.org/10.1007/s10291-018-0710-5

[30] Mendez Astudillo, J., Lau, L., Tang, Y.-T., & Moore, T. (2018). Analysing the Zenith Tropospheric Delay Estimates in On-line Precise Point Positioning (PPP) Services and PPP Software Packages. *Sensors*, *18(2)*, 580. https://doi.org/10.3390/s18020580

[31] Pan, L., & Guo, F. (2018). Real-time Tropospheric Delay Retrieval with GPS, GLONASS, Galileo and BDS Data. *Scientific Reports*, *12*, 17067. https://doi.org/10.1038/s41598-018-35155-3

[32] Byun, S. H., Hajj, G. A., & Young, L. E. (2002). Development and Application of GPS Signal Multipath Simulator. *Radio Science*, *37*(6), 10-1–10-23. https://doi.org/10.1029/2001RS002549

[33] Han, K., Tang, C., & Deng, Z. (2019). A New Method for Multipath Filtering in GPS Static High-precision Positioning. *Sensors*, *19(12)*, 2704. https://doi.org/10.3390/s19122704

[34] Heng, L., Gao, G. X., Walter, T., & Enge, P. (2010). GPS Ephemeris Error Screening and Results for 2006–2009. *Proceedings of the 2010 International Technical Meeting of the Institute of Navigation (ION ITM 2010)*, USA, 1014–1022. https://www.ion.org/publications/abstract.cfm?articleID=8881

[35] Montenbruck, O., Steigenberger, P., & Aicher, M. (2021). A Long-term Broadcast Ephemeris Model for Extended Operation of GNSS Satellites. *Navigation, Journal of the Institute of Navigation*, *68(1)*, 199–215. https://doi.org/10.1002/navi.404

[36] Langley, R. B. (1999). Dilution of Precision. *GPS World*, *5*, 52–59. http://www2.unb.ca/gge/Resources/gpsworld.may99.pdf

[37] Santerre, R., Geiger, A., & Banville, S. (2017). Geometry of GPS Dilution of Precision: Revisited. *GPS Solutions*, *21(4)*, 1747–1763. https://doi.org/10.1007/s10291-017-0649-y

[38] Ma, G., Gao, W., Li, J., Chen, Y., & Shen, H. (2014). Estimation of GPS Instrumental Biases from Small Scale Network. *Advances in Space Research*, *54(5)*, 871–882. https://doi.org/10.1016/j.asr.2013.01.008

[39] Zhilinskiy, V., Gagarina, L., Ishkova, T., Petrov, E., & Petrova, A. (2019). Software Package for Solving Navigation Problem Using Systematic Instrumental Error Correction. *Proceedings of the 2019 IEEE Conference of Russian Young Researchers in Electrical and Electronic Engineering (EIConRus 2019)*, Russia, 1871–1875. https://doi.org/10.1109/EIConRus.2019.8657157

[40] Specht, C. (2007). *GPS System*. Publishing House of the Bernardinum. https://www.researchgate.net/profile/Cezary-Specht/publication/260006261_System_GPS/links/0deec52f1fa70440f4000000/System-GPS.pdf (in Polish)

[41] Barros, M. S. S., Rosa, L. C. L., Walter, F., & Alves, L. H. P. M. (1999). Global Positioning System: A Methodology for Modelling the Pseudorange Measurements. *Advances in Space Research*, *23(8)*, 1529–15232. https://doi.org/10.1016/s0273-1177(99)00308-7

[42] Barros, M. S. S., Rosa, L. C. L., Walter, F., & Méndez, D. (2001). GPS: Statistical Models to Reproduce the Pseudoranges in Different Scenarios and their Reliability Evaluation. *Advances in Space Research*, *28(1)*, 227–232. https://doi.org/10.1016/S0273-1177(01)00348-9

[43] Koyama, Y., & Tanaka, T. (2010). Improvements in Accurate GPS Positioning Using Time Series Analysis. *Proceedings of the SICE Annual Conference 2010 (SICE 2010)*, Taiwan, 282–285. https://doi.org/10.9746/jcmsi.4.283

[44] Belabbas, B., Hornbostel, A., & Sadeque, M. Z. (2005). Error Analysis of Single Frequency GPS Measurements and Impact on Timing and Positioning Accuracy. *Proceedings of the 2nd Workshop on Positioning, Navigation and Communication 2005 (WPNC 2005) and 1st Ultra-wideband Expert Talk 2005 (UET 2005)*, Germany, 81–86. https://citeseerx.ist.psu.edu/viewdoc/download?doi=10.1.1.519.1622&rep=rep1&type=pdf

[45] Belabbas, B., Petitprez, F., & Hornbostel, A. (2005). UERE Analysis for Static Single Frequency Positioning Using Data of IGS Stations. *Proceedings of the 2005 National Technical Meeting of the Institute of Navigation (ION NTM 2005)*, USA, 310–319. https://www.ion.org/publications/abstract.cfm?articleID=5998

[46] Federici, B., Giacomelli, D., Sguerso, D., Vitti, A., & Zatelli, P. (2013). A Web Processing Service for GNSS Realistic Planning. *Applied Geomatics*, *5*(1), 45–57. https://doi.org/10.1007/s12518-011-0058-9

[47] Gandolfi, S., & La Via, L. (2011). SKYPLOT_DEM: A Tool for GNSS Planning and Simulations. *Applied Geomatics*, *3*(1), 35–48. https://doi.org/10.1007/s12518-011-0045-1

[48] Nowak, A. (2017). Dynamic GNSS Mission Planning Using DTM for Precise Navigation of Autonomous Vehicles. *The Journal of Navigation*, *70*(3), 483–504. https://doi.org/10.1017/S0373463316000679

[49] Specht, M., Specht, C., Dąbrowski, P., Czaplewski, K., Smolarek, L., & Lewicka, O. (2020). Road Tests of the Positioning Accuracy of INS/GNSS Systems Based on MEMS Technology for Navigating Railway Vehicles. *Energies*, *13*(17), 4463. https://doi.org/10.3390/en13174463

[50] Spilker Jr., J. J., Axelrad, P., Parkinson, B. W., & Enge, P. (1996). *Global Positioning System: Theory and Applications*. AIAA. https://arc.aiaa.org/doi/book/10.2514/4.866388

Metrol. Meas. Syst., Vol. 29 (2022), No. 1, pp. 17–36
DOI: 10.24425/mms.2022.138549

[51] Teunissen, P. J. G., & Odijk, D. (1997). Ambiguity Dilution of Precision: Definition, Properties and Application. *Proceedings of the 10th International Technical Meeting of the Satellite Division of the Institute of Navigation (ION GPS 1997)*, USA, 891–899. https://www.ion.org/publications/abstract.cfm?articleID=2811

[52] Odijk, D., & Teunissen, P. J. G. (2008). ADOP in Closed Form for a Hierarchy of Multi-frequency Single-baseline GNSS Models. *Journal of Geodesy*, *82*, 473–492. https://doi.org/10.1007/s00190-007-0197-2

[53] Wang, K., Teunissen, P. J. G., & El-Mowafy, A. (2020). The ADOP and PDOP: Two Complementary Diagnostics for GNSS Positioning. *Journal of Surveying Engineering*, *146*(2), 04020008. https://doi.org/10.1061/(ASCE)SU.1943-5428.0000313

[54] Specht, M. (2020). A Statistical Distribution Analysis of Navigation Positioning System Errors – Issue of the Empirical Sample Size. *Sensors*, *20*(24), 7144. https://doi.org/10.3390/s20247144

[55] Specht, M. (2021). Consistency Analysis of Global Positioning System Position Errors with Typical Statistical Distributions. *The Journal of Navigation*, *74*(6), 1201–1218. https://doi.org/10.1017/S0373463321000485

[56] Specht, M. (2021). Consistency of the Empirical Distributions of Navigation Positioning System Errors with Theoretical Distributions – Comparative Analysis of the DGPS and EGNOS Systems in the Years 2006 and 2014. *Sensors*, *21*(1), 31. https://doi.org/10.3390/s21010031

[57] Specht, M. (2021). Determination of Navigation System Positioning Accuracy Using the Reliability Method Based on Real Measurements. *Remote Sensing*, *13*(21), 4424. https://doi.org/10.3390/rs13214424

[58] Yin, M.-L., & Arellano, R. (2012). A Risk Analysis Framework on GPS User Range Accuracy. *Proceedings of the 2012 Annual Symposium on Reliability and Maintainability (RAMS 2012)*, USA, 1–6. https://doi.org/10.1109/RAMS.2012.6175502

[59] NAVCEN (2011). *Interface Specification IS-GPS-200F*. NAVCEN. https://www.navcen.uscg.gov/pdf/IS-GPS-200F.pdf

[60] Heng, L., Gao, G. X., Walter, T., & Enge, P. (2011). Statistical Characterization of GPS Signal-In-Space Errors. *Proceedings of the 2011 International Technical Meeting of the Institute of Navigation (ION GNSS 2011)*, USA, 312–319. https://www.ion.org/publications/abstract.cfm?articleID=9472

[61] Specht, C., Mania, M., Skóra, M., & Specht, M. (2015). Accuracy of the GPS Positioning System in the Context of Increasing the Number of Satellites in the Constellation. *Polish Maritime Research*, *22(2)*, 9–14. https://doi.org/10.1515/pomr-2015-0012

[62] Grewal, M. S., Weill, L. R., & Andrews A. P. (2007). *Global Positioning Systems, Inertial Navigation, and Integration*. John Wiley & Sons, Inc. https://www.wiley.com/en-us/Global+Positioning+Systems%2C+Inertial+Navigation%2C+and+Integration%2C+2nd+Edition-p-9780470099711

[63] Deakin, R. E., Hunter, M. N., & Karney, C. F. F. (2010). The Gauss–Krüger Projection. *Proceedings of the 23rd Victorian Regional Survey Conference*, Australia, 1–20. https://www.academia.edu/27744389/THE_GAUSS_KR%C3%9CGER_PROJECTION

[64] Norman, L. J., Kotz, S., & Balakrishnan, N. (1994). *Continuous Univariate Distributions*. John Wiley & Sons, Inc. https://www.wiley.com/en-us/Continuous+Univariate+Distributions%2C+Volume+1%2C+2nd+Edition-p-9780471584957

Mariusz Specht received the Ph.D. degree from the Polish Naval Academy, Poland, in 2019. He is currently an Assistant Professor at Gdynia Maritime University. He has authored or coauthored 86 peer-reviewed publications, including 50 articles in JCR-listed journals. He is the leader in the National Centre for Research and Development (Poland) grant entitled "Innovative autonomous unmanned bathymetric monitoring system for shallow waterbodies". His current research interests include the applications of GNSS systems in geodesy, hydrography and navigation.

View publication stats